Eur. Phys. J. D **26**, 27–32 (2003)
DOI: 10.1140/epjd/e2003-00200-0

THE EUROPEAN PHYSICAL JOURNAL D

Effects of electric fields and collisions on highly excited rubidium atoms

N.I. Hammer and R.N. Compton[a]

Departments of Chemistry and Physics, The University of Tennessee, Knoxville TN 37996, USA

Received 12 November 2002 / Received in final form 11 March 2003
Published online 8 July 2003 –

Abstract. The effects of static and pulsed electric fields on the multiphoton ionization (MPI) of rubidium atoms at both low (atomic beam) and high (heat pipe) densities are studied using tunable OPO lasers. Two-photon excitation of *np* states is induced by the external electric field at both low and high densities. In addition, *np* signal is also seen at very low electric fields in the heat pipe, providing evidence for collision mixing as well as field mixing. At low Rb densities strong resonance features are observed in the energy region between the zero field limit (*IP*) and the field ionization limit. In addition, collisional detachment and charge transfer between excited *ns* and *nd* Rb Rydberg states and nozzle-jet cooled polar molecules (acetonitrile and acetone) are studied under crossed-beam conditions. The formation of dipole bound anions for acetone is only seen under nozzle jet expansion conditions and the maximum in the Rydberg electron transfer (RET) rate *versus* n depends upon the expansion gas ($n_{\max}$ increases in the order H_2, He, Ne, Ar, Xe). For acetone (low dipole moment and large $n_{\max}$), collisional detachment dominates the charge transfer, whereas for acetonitrile (high dipole moment and low $n_{\max}$), charge transfer is seen to dominate the creation of Rb^+.

PACS. 33.80.Rv Multiphoton ionization and excitation to highly excited states (e.g., Rydberg states) – 34.60.+z Scattering in highly excited states (e.g., Rydberg states) – 34.70.+e Charge transfer

1 Introduction

The chemical and physical properties of atoms in high Rydberg states has been a topic of intense study for many years [1,2]. The ground and excited states of an atom are termed Rydberg states if the energy levels can be described as a quasi-hydrogenic "one-electron" atom and the energy levels relative to the ground state follow the Rydberg formula

$$E_{n,l} = IP_A - \left(R_A/n^{*2}\right) \tag{1}$$

where IP_A represents the ionization potential of the atom, R_A is the Rydberg constant for the atom and n^* is the effective principal quantum number ($n^* = n - \delta_l$, with δ_l being the l-dependent quantum defect). The various n and l states are easily obtained either by a single or multiphoton process. In this paper we discuss the effects of static and pulsed electric fields and collisions with two polar molecules on the excitation and decay of atoms in high n states with $l = 0$ and 2. The presence of a dc electric field produces Stark-mixing of these excited states and effectively lowers the ionization potential of an atom [1,2]. A simplified treatment of the field effects follows: the potential energy for a Rydberg electron in the presence of an electric field can be approximated by

$$V(r) = -e^2/r - eEr \tag{2}$$

where e is the charge on an electron, r is the distance of the electron from the core, and E is the magnitude of the external electric field. As the field is increased the effective ionization potential is lowered since the "zero-field" high Rydberg states are in the continuum and are field-ionized. Figure 1 shows the electric field modified potential energy diagram for rubidium. The ionization potential is lowered to the "effective ionization potential" by the amount

$$V_{\text{lowering}} = 2e^{3/2}E^{1/2} \tag{3}$$

Rydberg states with energy above this new effective potential escape over the barrier and those below $V_{\max}$ can only tunnel through the potential barrier. For the time of observation of most experiments, tunneling is observed only for those states close to the top of the barrier.

The electric field can be applied either during the process of excitation (dc field) or as a pulsed field after the excitation has occurred. Both conditions are described in this study. In addition to lowering the effective ionization limit, resonance features have been reported in the region above the zero field threshold [3]. Considerable experimental and theoretical interest has been devoted

[a] e-mail: rcompton@utk.edu

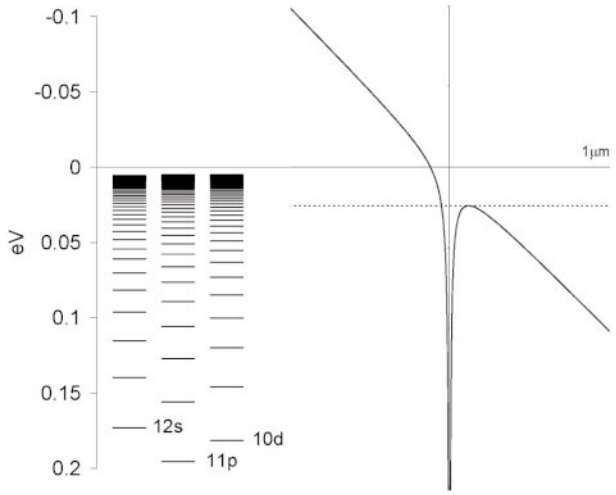

Fig. 1. Electric field modified potential energy diagram for rubidium showing field ionization of high Rydberg states over the top of the barrier at $V_{\max}$.

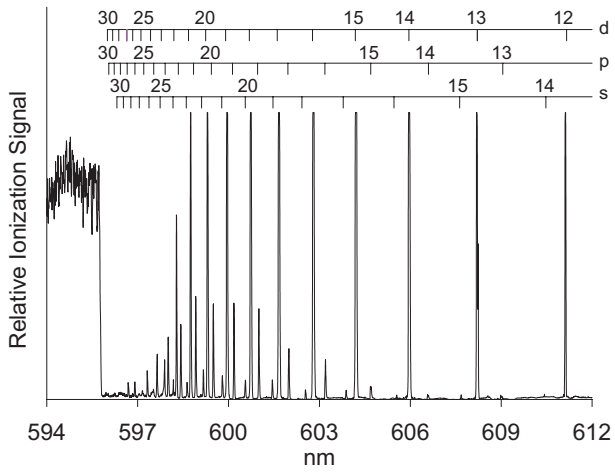

Fig. 2. Typical MPI spectrum of rubidium atoms in a dc electric field at low densities. The nd states below $n = 21$ are saturated.

to these above-threshold resonances. Field induced resonances have also been seen in the region between the zero field threshold (IP) and the field ionization limit [4,5]. These studies will be revisited below.

The effects of a dc electric field on multiphoton ionization of an alkali atom (cesium) have been reported previously [5,6]. In addition to the well-known field-ionization effects, a dc field was seen to induce access to the dipole forbidden two-photon np series. Previously, Zhang *et al.* [7] observed ionization through two-photon excited np states of sodium at high densities (heat pipe). The origin of this forbidden excitation was uncertain and is one of the subjects of this study.

We also report studies of crossed beam collisional ionization of these same Rb ns and nd Rydberg states by seeded nozzle jet expansions of polar molecules of high (acetonitrile, 3.94 D) and moderate (acetone, 2.88 D) dipole moment. The formation of dipole bound anions through Rydberg electron transfer (RET), is seen to compete favorably with collisional ionization in certain regions of n. The maximum in the RET rate ($n_{\max}$) is determined primarily by the electron binding energy, however a dependence of $n_{\max}$ on the expansion gas is observed for acetone.

2 Experimental procedure

The output of a tunable OPO laser (Continuum Sunlite or single mode Mirage) pumped by the third harmonic ($\lambda = 355$ nm) of the fundamental ($\lambda = 1064$ nm) of a Nd:YAG laser (Continuum Powerlite) was transmitted through a heat-pipe oven containing rubidium vapor for high density studies and into a rubidium atomic beam apparatus for studies at low density. The heat pipe was 25 cm long with a 2 cm internal diameter. The rubidium pressure in the heat pipe and the density of the atomic beam were controlled by the temperature (20–200 °C) of each. The Continuum Sunlite OPO and Mirage OPO have narrow linewidths (approximately 0.20 and 0.02 cm^{-1}, respectively), which make them ideally suited to study the high Rydberg states of alkali atoms through multiphoton excitation/ionization. The absolute wavelength of the pulsed laser was determined to within 0.001 nm with a Burleigh wavemeter model WA-4500-0. The ionization signal from the heat pipe was collected on a biased insulated collector wire. The wire was positioned to be off center but along the active region of the heat pipe. The ions or electrons in the atomic beam apparatus were detected using a time-of-flight mass spectrometer and a dual-microchannel plate electron multiplier. A voltage applied to a metal pusher plate was used to accelerate the ions. In some studies the pusher voltage was continuous, but in others it was pulsed with a 1 μs delay and 5 μs duration. Thus 2-photon excitation could be studied with or without the influence of an external electric field. For the charge transfer experiments an RM Jordan PSV pulsed supersonic valve (model C-211) was used to pulse a seeded jet of molecules into the region at right angles to the excited rubidium beam. After a reaction time of approximately 2 μs the resulting negative ions or rubidium cations were extracted with a pulsed voltage. The ionization signal from both the heat pipe and atomic beam setup was observed as either a negative or positive signal, depending on whether electrons, negative ions, or positive ions were being collected. The positive or negative voltage pulses were displayed on a digital oscilloscope, averaged by a boxcar integrator (Stanford Research Systems model SR250), and recorded by a data acquisition computer program. Negative or positive ions in the atomic beam experiments were analyzed with the 0.65 meter time-of-flight mass spectrometer.

3 Results and discussion

Figures 2 and 3 show typical 2+1 multiphoton ionization spectra for rubidium. Figure 2 was recorded in the

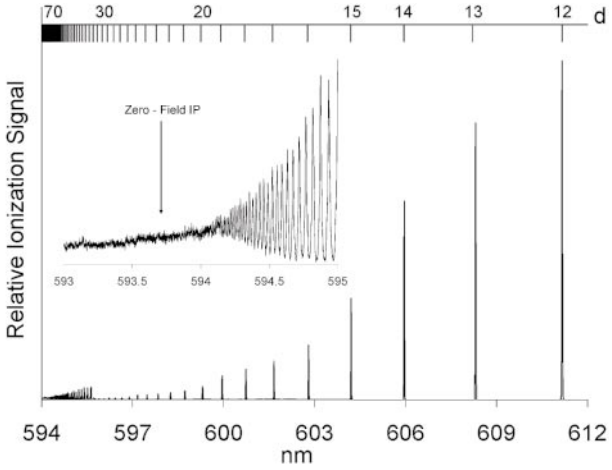

Fig. 3. Typical MPI spectrum of rubidium atoms in a pulsed electric field at low densities.

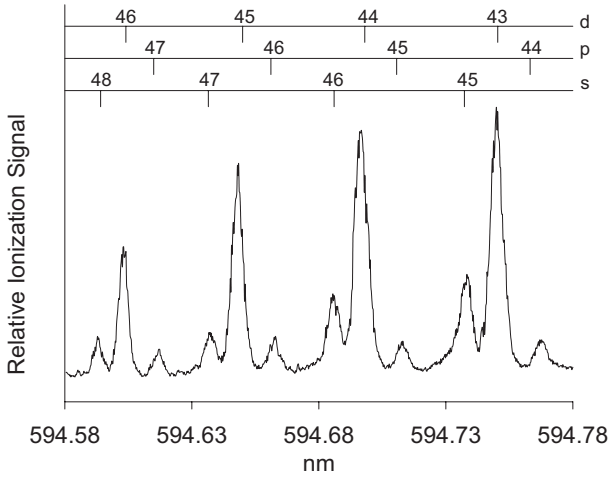

Fig. 4. High-n Rydberg states of rubidium obtained in a heat pipe with a small electric field (∼10 V on wire).

atomic beam apparatus at a constant dc electric field of 35000 V/m and shows many of the possible Rydberg states ($n > 12$). One can see the prominent 2+1 MPI nd transitions, smaller ns and forbidden np transitions near the ionization potential, and the field-induced ionization signal. The two-photon zero field IP is 593.63 nm. The ns transitions are small because of their small photoionization cross-sections. Signal from most of the nd transitions below $n = 21$ are saturated. Figure 3 was recorded with a pulsed electric field of 35000 V/m. The nd signal is seen to fall off roughly as n^{*-7} as seen previously [5] and is accounted for by a decreasing excitation probability (roughly as n^{*-3}) as well as decreasing photoionization cross-section.

3.1 Ionization in high density heat pipe

In the atomic beam experiment the lower nd transitions are more prominent relative to ns or np states due to their larger photoionization cross-sections. However, in the heat pipe collisional ionization also plays a role, and as a result ionization of *both* higher ns and nd Rydberg states can be readily seen. It was also observed that the symmetry forbidden two-photon excited np states were prominent at high n and that increasing the electric field in the heat pipe or atomic beam experiment increased the np signal. Shown in Figure 4 is a typical spectrum obtained in the heat pipe showing the ns, np, and nd states. Figure 5 shows the ratio of the signal intensities of the $41p$ and the $41s$ states as the voltage on the collection wire (and hence the electric field in the heat pipe) is increased. The absolute intensity of the ns transition is not affected by the presence of an electric field and therefore such a ratio was used in order to compensate for any variations in laser power or alkali vapor pressure. It appears that the increase in np signal (relative to a nearby ns state) is approximately linear with respect to the applied voltage with a non-zero intercept. The non-zero intercept is attributed to population of np states through collisions.

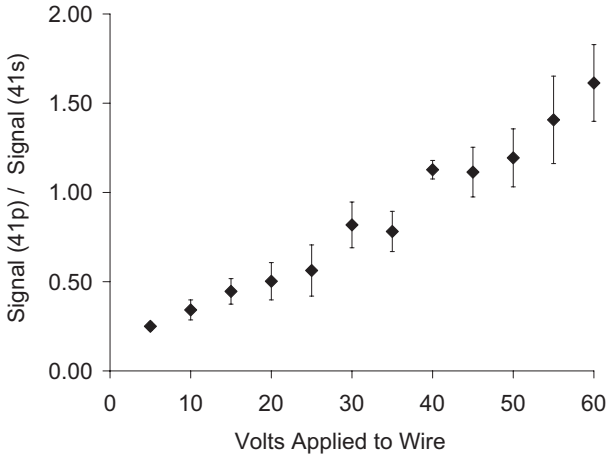

Fig. 5. Ratio of intensities of the $41p$ and the $41s$ states of rubidium as a function of applied voltage.

3.2 Ionization in low density atomic beam

Results for the atomic beam experiment were similar to those obtained in the heat pipe except that excitation and ionization *via* collisions was absent. Four MPI spectra taken at various increasing electric field strengths are shown in Figure 6. The forbidden np transitions were observed *only* through the application of a constant electric field. The intensity of the np transitions increases with applied electric field, but then levels off and becomes unaffected by further increases in field strength. Interestingly, while the np signal remains constant with ever-increasing field the nd signal decreases. Presumably, the magnetic sublevels of the nd states are spreading out and becoming more diffuse.

When a dc electric field was applied to accelerate the ions distinct resonances were observed in the region between the two-photon IP and the field induced ionization limit. Figure 2 shows such resonances. Similar resonances have been seen in potassium [3], rubidium [4], and cesium [5]. It was found that these resonances also depend

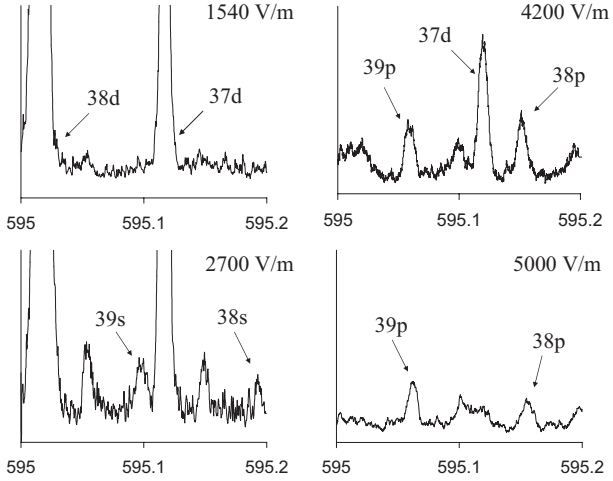

Fig. 6. Variation of high ns, np, and nd Rydberg states with increasing constant electric field.

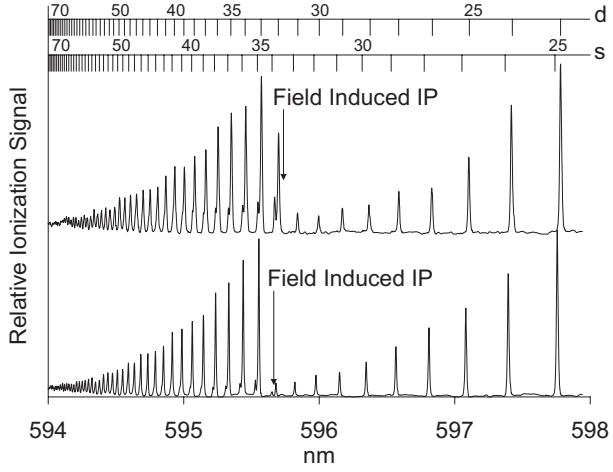

Fig. 7. Three-photon and field-ionized ns and nd Rydberg states at 37500 V/m (top) and 35000 V/m (bottom). The dashed line shows the calculated field induced ionization limit.

upon the direction of the plane of polarization of the laser relative to the direction of electric field, in a manner similar to that reported earlier for cesium [5]. These features are clearly field-induced as shown by measurements under pulsed field conditions, *i.e.* field ionization occurs from well-derived n_l states produced under zero field conditions. Figure 7 shows the falling off of the nd series as the field-induced limit is approached when pulsing the electric field 2 μs after the states are created. Interesting features appear in the region near the field ionization threshold. Note that the transition from the three-photon ionization to two-photon excitation/field ionization is not totally abrupt. The nd level just below the field ionization limit appears to be due to *both* tunneling and two-photon resonant three-photon ionization. Tunneling appears to be even more dramatic for the onset of ns levels in this region. Ionization of ns states is primarily through field ionization, however, it would appear that transmission through the coulomb barrier is greater for ns states than nd states. This could be accounted for by the absence of a centrifugal barrier for ns states, which would be present for the nd states.

3.3 Atomic beam-molecular jet collisions

The interaction of Rydberg atoms with atomic and molecular targets has been well studied. A review of the many aspects of this interaction can be found in numerous chapters of the book edited by Stebbings and Dunning [2]. In this work we examine the collisions of Rydberg atoms with molecules which are known to support a dipole-bound anion. All molecules with dipole moments above ∼2.5 D are expected to form a stable dipole-bound anion. A number of recent reviews summarize this active field of research [8–10]. In this work, collisions between excited (ns, nd) Rb atoms and a nozzle jet of rare gas as well as a jet of two polar molecules [CH_3CN (μ = 3.92 D) and $(CH_3)_2CO$ (μ = 2.88 D)] were studied under crossed-beam conditions. These two polar molecules were chosen to represent strongly (EA ∼20 meV) and weakly bound (EA ∼3 meV) dipole bound anions, respectively. Rubidium atoms in an atomic beam were excited by two-photons to ns and nd states using the OPO laser as discussed above. A pulsed nozzle jet of rare gas or polar molecules/rare gas mixtures was introduced through an RM Jordan PSV pulsed supersonic valve (model C-211) and crossed and interacted with the excited atoms for a period of time, t (typically 2 μs), after which the positive or negative ions were pulsed down the flight tube of the TOF mass spectrometer and analyzed. Figure 8a shows a typical scan of Rb^+ ion signal without the presence of any collision gas. As shown earlier in Figure 3, only signal due to (2+1) MPI of nd Rb Rydberg states with the abrupt onset at the field ionization threshold is indicated. Ionization due to ns states is also seen near this onset as discussed earlier. Figure 8b shows the Rb^+ ion signal resulting from collisions with acetone seeded in a jet of He. Most of the ionizing collisions are believed to be due to the presence of acetone in the nozzle jet. Notice the continuity of signal through the field ionization threshold and the appearance of ns states below this limit. Figure 8c shows the dipole bound negative ion signal. The absence of a clear peak in the Rb^+ signal is clear evidence that collisional detachment dominates RET in this region of n. A similar set of data is shown in Figure 9 for the case of the highly polar molecule, acetonitrile (μ = 3.92 D). Again, collisional ionization is larger for high ns and nd states, however, RET is seen to clearly dominate the collisions in the region of low ns and nd. These experiments emphasize the importance of a better theoretical understanding of the interaction of Rydberg atoms and polar molecules, especially the dynamic competition between collisional ionization and dipole anion formation. The need for further theory in describing the dynamics of RET formation in polar molecules is presented in Figure 10. This figure shows that n^*_{max} for the formation of the acetone dipole anion is dependent on the carrier gas in the nozzle jet. This variation of RET rate with expansion gas is likely due to the changing velocity of the acetone

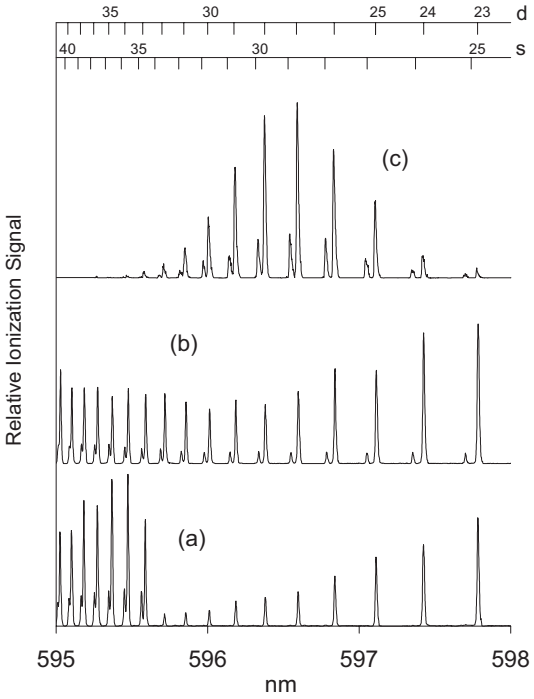

Fig. 8. Rb^+ ionization signal with no gas jet (a), Rb^+ ionization signal with acetone gas jet (b), and acetone ($CH_3COCH_3^-$) dipole-bound anion signal (c).

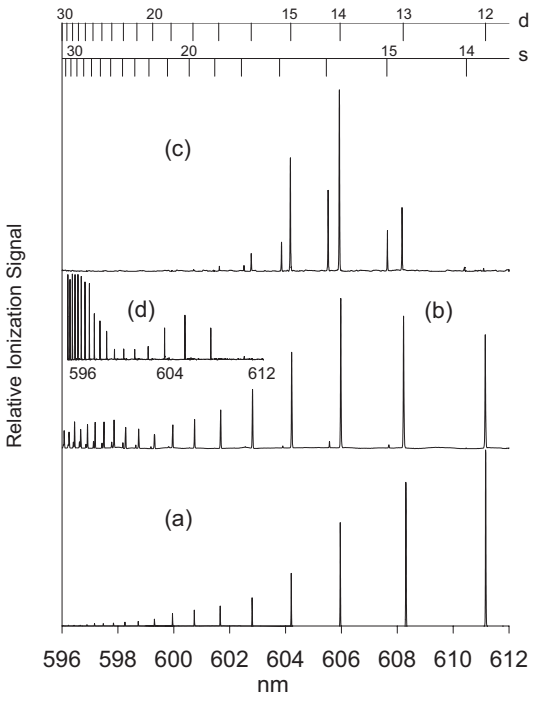

Fig. 9. Rb^+ ionization signal with no gas jet (a), Rb^+ ionization signal with acetonitrile gas jet (b), acetonitrile (CH_3CN^-) dipole-bound anion signal (c), and magnification of ns Rb^+ states created from RET (d).

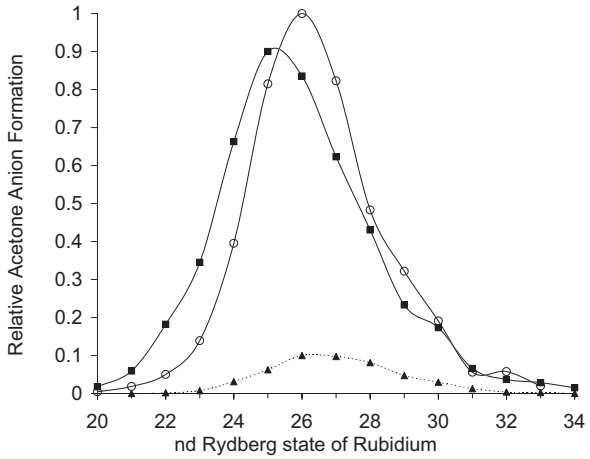

Fig. 10. Negative ion signal of acetone with the carrier gases He (squares), Ar (circles), and Xe (triangles).

molecules entrained in the rare gas as well as rotational cooling. It should be emphasized that acetone negative ions are only seen under nozzle jet expansion conditions. This could be partly related to the need for relative velocities in order to allow separation of the alkali cation-dipole anion pair. However, dipole-bound anions of acetonitrile and other high dipole moment molecules are easily seen without seeding. The importance of nozzle jet expansion was pointed out earlier [8] and could be partly due to the necessity to rotationally cool the acetone in order to allow for binding. Acetone molecules at room temperature will populate sufficiently high rotational states such that rapid autodetachment of the electron occurs from the weakly bound negative ions of acetone. At lower temperatures the majority of the molecules are in the lowest energy rotational states. However, as the temperature is increased the higher rotational states become populated and charge transfer to form the dipole bound anion becomes less likely. This is not the case for acetonitrile, which has a much larger electron affinity that is well above the rotational energy levels that are populated even at higher temperatures. It is believed that the molecules in the nozzle jet expansion are cooled to a rotational temperature range of about 5–20 K, depending upon the carrier gas employed. Argon and helium effectively cool acetone to lower temperatures compared to xenon. Even at this temperature a significant number of molecules are populating rotational levels close in energy to the electron affinity of acetone. This might explain the larger collisional cross-section for detachment in the case of acetone compared to that of CH_3CN. The electron is transferred creating Rb^+ in both cases but in acetone rotations quickly detach it. The rotational states populated in CH_3CN, however, are not sufficient to do so. The poor ability of xenon to cool along with its slower velocity would yield much fewer anions than argon or helium, as shown in Figure 10.

4 Conclusions

The present study demonstrates that resonantly enhanced 2+1 multiphoton ionization of rubidium atoms through the two-photon forbidden np Rydberg states occurs primarily as a result of state mixing induced by the presence of an external electric field. At high rubidium pressures (heat pipe) there is also evidence for collisional mixing of forbidden and allowed states leading to ionization. Specifically, the non-zero intercept in Figure 5 provides evidence that there is some collisionally-induced state mixing. Similar results were reported in our earlier studies of sodium [7], and are fully explained by the conclusions reported herein. In the heat pipe experiments, collisions primarily account for the ionization of the resonantly excited nl states. This is apparent due to the presence of strong ns ionization signal at high densities. Signals resulting from ns states are very weak at low densities. MPI *via* the 2+1 ns intermediate state is small because the photoionization cross-section for the ns states is very low in comparison to that of the nd states. On this basis, one would also conclude that the ionization signals attributed to forbidden np states are also a result of collisions.

Data from the pulsed electric field ionization studies of high Rydberg ns and nd states are seen generally to obey the field ionization model as embodied in equation (3). Evidence is also presented for tunneling near the top of the Coulomb barrier. A higher tunneling rate is observed for the ns states than the nd states, indicative of the role (*i.e.*, absence for ns states) of centrifugal barriers as well. In the dc field ionization studies, rich structure is seen in the energy region between the field ionization limit and zero field ionization thresholds. The above threshold resonances observed here are very similar to others seen previously for potassium [3], rubidium [4], and cesium [5] and await a detailed theoretical interpretation.

It is apparent from the Rydberg atom/polar molecule experiments that collisional ionization dominates the ionization of the Rydberg atom at higher n whereas at lower n RET dominates. The detailed mechanisms for electron transfer to a dipole is still not well understood. Lighter carrier gases such as helium and neon lead to electron transfer at lower n, whereas heavier gases such as krypton and xenon exhibit charge transfer maxima at higher values of n. The lighter carrier gases give rise to higher velocities for the entrained molecules than the heavier gases. A full account of this will be published in a forthcoming paper [11]. A proper theoretical treatment of Rydberg atom/polar molecule interactions will have to include the dynamical interplay between collisional detachment and RET. The considerations of Clary [12] on rotationally adiabatic potentials of continuum dipole anion states may provide a starting point for such a theory.

This research was supported by the National Science Foundation.

References

1. T. Gallagher, *Rydberg Atoms* (Cambridge University Press, Cambridge, 1983)
2. R.F. Stebbings, F.B. Dunning, *Rydberg States of Atoms and Molecules* (Cambridge Press, 1983)
3. R.R. Freeman, N.P. Economou, G.C. Bjorklund, Phys. Rev. Lett. **41**, 1463 (1978)
4. Y. Sato, Y. Teraoka, J. Murakami, in *International Seminar On Highly States of Atoms and Molecules*, edited by S.S. Kano, M. Matsuzawa (Fuji-Yoshida, Japan, 1986)
5. C.E. Klots, R.N. Compton, in *Multiphoton Processes*, edited by P. Lambropoulos, S.J. Smith (Springer-Verlag, Berlin, 1984)
6. C.E. Klots, R.N. Compton, Phys. Rev. A **31**, 525 (1985)
7. J. Zhang, P. Lambropoulos, D. Zei, R.N. Compton, J.A.D. Stockdale, Z. Phys. D **23**, 219 (1992)
8. C. Desfrancois, H. Abdoul-Carime, J.P. Schermann, Int. J. Mod. Phys. **10**, 1339 (1996)
9. R.N. Compton, in *The Role of Rydberg States in Spectroscopy and Photochemistry*, edited by C. Sandorfy (Kluwer Academic, 1999)
10. R.N. Compton, N.I. Hammer, in *Advances in Gas-Phase Ion Chemistry*, edited by N. Adams, L. Babcock (Elsevier Science, 2001), Vol. 4
11. N.I. Hammer, K. Diri, K.D. Jordan, C. Desfrancois, R.N. Compton, to be pubished
12. D.C. Clary, J. Phys. Chem. **92**, 3173 (1988)